Chem. Res. Chin. Univ., 2015, 31(5), 708—711 doi: 10.1007/s40242-015-5136-9

Synthesis and Electrochemical Properties of Highly Crystallized CuV_2O_6 Nanowires

HU Fang[1,2], LI Malin[2], WEI Yingjin[2], DU Fei[2], CHEN Gang[2] and WANG Chunzhong[2*]

1. School of Materials Science and Engineering, Shenyang University of Technology, Shenyang 110870, P. R. China;
2. Key Laboratory of Advanced Batteries Physics and Technology, Ministry of Education, College of Physics, Jilin University, Changchun 130012, P. R. China

Abstract CuV_2O_6 nanowires were prepared *via* a simple hydrothermal route using NH_4VO_3 and $Cu(NO_3)_2$ as starting materials. The structures and electrochemical properties of CuV_2O_6 nanowires were characterized by means of X-ray diffraction(XRD), scanning electron microscopy(SEM) and transmission electron microscopy(TEM). The results show that the CuV_2O_6 nanowires are about 100 nm in width and single crystalline grown along [001] direction. CuV_2O_6 nanowires delivered a high initial discharge capacity of 435 and 351 mA·h/g at current densities of 50 and 100 mA·h/g, respectively. The electrochemical kinetics of the CuV_2O_6 nanowires was also investigated by means of electrochemical impedance spectroscopy(EIS) and the poor rate performance was observed, which may be attributed to the low ion diffusion coefficient of the CuV_2O_6 nanowires.

Keywords CuV_2O_6; Nanowire; Electrochemical property

1 Introduction

Vanadium bronzes have displayed very interesting transport and magnetic properties, including charge and spin ordering, metal-insulator transitions and superconductivity[1—3]. Besides these, the catalysis and electrochemical properties of vanadium bronzes have also been discussed[4—6]. Vanadium bronzes have shown several intrinsic advantages, such as large energy density and good thermal stability[7,8], which are benefit for their potential applications as cathode materials for primary or secondary lithium batteries[9—11]. For example, primary lithium batteries using $Ag_2V_4O_{11}$(SVO) as the cathode materials have been used commercially in the implantable cardioverter defibrillators(ICDs)[9].

Cooper vanadium bronzes(CVO) include CuV_2O_6, $Cu_{2.33}V_4O_{11}$, $Cu_{1.1}V_4O_{11}$ and so on, and the electrochemical properties of them have been studied for a long time[12,13]. Among the present CVO systems, CuV_2O_6 can deliver the highest specific capacity and energy density[14]. However, the synthesizing technique also plays an important role in the electrochemical performance of CuV_2O_6. Wei *et al.*[7] synthesized CuV_2O_6 *via* co-precipitation method, and the first discharge capacity of 379 mA·h/g was achieved in the potential region of 1.5—4.0 V. After 30 cycles, the discharge capacity of CuV_2O_6 was decreased to 160 mA·h/g. Cao *et al.*[15] synthesized CuV_2O_6 from V_2O_5 hydrogel and Cu_2O powder, and the first discharge capacity was 350 mA·h/g in the potential region of 2.0—4.0 V. After 20 cycles, the discharge capacity of CuV_2O_6 decreased to 210 mA·h/g. Wang *et al.*[16] prepared CuV_2O_6 by sol-gel method, which showed a first discharge capacity of 403 mA·h/g in the potential region of 1.5—4.0 V. After 30 cycles, the discharge capacity of CuV_2O_6 reduced to 150 mA·h/g. Herein, the single crystalline CuV_2O_6 nanowires were synthesized *via* hydrothermal method using NH_4VO_3 and $Cu(NO_3)_2$ as raw reagents. The cycle performance and electrochemical kinetics of the as-prepared CuV_2O_6 nanowires were also investigated.

2 Experimental

2.1 Method

All the reagents were of analytical grade and used without further purification. In a typical procedure, 0.234 g of NH_4VO_3 was added to a beaker with 20 mL of distilled water and the solution was stirred at 80 °C for 30 min to make sure NH_4VO_3 has dissolved completely. 0.241 g of $Cu(NO_3)_2$ was dissolved in 20 mL of distilled water. Then, the $Cu(NO_3)_2$ solution was slowly dropped into the NH_4VO_3 solution under stirring at 80 °C, with a yellow precipitate formed immediately. After continuous stirring at 80 °C for 30 min, the yellow suspension was transferred into an orange suspension, which was then poured into a 40 mL Teflon-lined stainless steel autoclave and maintained at 210 °C for 18 h. After the hydrothermal reaction completed, the autoclave was cooled to room temperature in air. The orangey powders obtained were collected and washed several times by distilled water and ethanol, respectively. Last, the powders were dried at 80 °C to obtain the final product.

*Corresponding author. E-mail: wcz@jlu.edu.cn

Received April 3, 2015; accepted June 12, 2015.

Supported by the National Basic Research Program of China(No.2015CB251103), the National Natural Science Foundation of China(No.51472104) and the Development Program of Science and Technology of Jilin Province, China(No.20140101093JC).

2.2 Structural and Electrochemcial Measurement

The crystal structure of the material was studied by means of X-ray diffraction on an XRD-7000 diffractometer equipped with Cu $K\alpha$ radiation. The morphology of the material was studied by a scanning electron microscope(SEM, JSM-6700F) at 5.0 kV. The microstructure was analyzed on a JEOL-3010 transmission electron microscope(TEM) at an accelerating voltage of 300 kV.

Electrochemical experiments were carried out using a coin battery cell with a metallic lithium foil served as the anode electrode. The cathode electrode was fabricated by blending the CuV_2O_6 active material(80%, mass fraction) with acetylene black(10%, mass fraction) and poly-vinylidenefluoride(PVDF, 10%, mass fraction). The slurry obtained was pasted on an Al foil and then dried in a vacuum oven. The electrolyte was 1 mol/L lithium hexafluorophosphate($LiPF_6$) dissolved in the mixture of ethylene carbonate(EC) and dimethyl carbonate (DMC)[V(EC):V(DMC)=1:1]. Galvonostatic charge-discharge cycling was performed with an automatic battery tester (Land-2100, China). Electrochemical impedance spectroscopy(EIS) was carried out by a Zaher Elektrik IM6e electrochemical analyzer in a frequency range from 1 MHz to 1 mHz.

3 Results and Discussion

Fig.1 shows the X-ray diffraction(XRD) pattern of the as-prepared material. The positions and relative intensities of all the diffraction peaks could be indexed well to those of the pure triclinic phase of CuV_2O_6 according to JCPDS No.30-0513. The lattice parameters of the material, a=0.9165 nm, b=0.3553 nm, c=0.6478 nm, α=92.3°, β=110.3°, γ=91.7°, are similar to those shown in the previous reports[14,15]. Strong and sharp diffraction peaks indicate that the as-prepared material is highly crystallized.

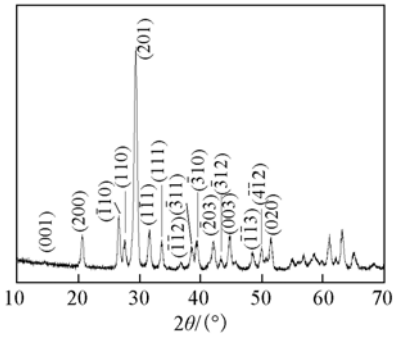

Fig.1 XRD pattern of the CuV_2O_6 sample

The SEM images of the CuV_2O_6 sample(Fig.2) show that the material is composed of wire-like particles with about 10 μm in length. Under a higher magnification, it can be seen that the average width of the nanowires is about 50—200 nm, the height of which is only about several tens of nanometers. The CuV_2O_6 nanowires were further investigated by means of TEM(Fig.3). Ma *et al.*[14] used HRTEM to investigate the CuV_2O_6 nanowire synthesized with NH_4VO_3 and $CuCl_2$ and reported that the nanowire was grown along [110] direction investigated by HRTEM. Herein, the result of selected area electron diffraction(SAED) indicates the growth direction of the material synthesized by NH_4VO_3 and $Cu(NO_3)_2$ is along [001] direction, which shows that different raw materials can result in different growth directions of CuV_2O_6 nanowires.

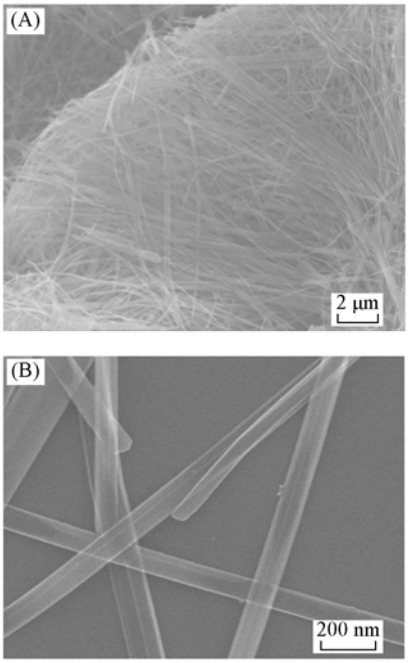

Fig.2 SEM images of CuV_2O_6 nanwires with low(A) and high(B) magnifications

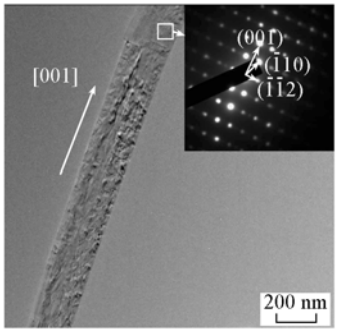

Fig.3 TEM image and SAED pattern(inset) of CuV_2O_6 nanowires

The charge-discharge cycling performance of the CuV_2O_6 nanowires was studied in the voltage window of 2.0—4.0 V. Fig.4(A) displays the charge-discharge potential profiles of the samples during the first two cycles with the current density of about 50 mA/g. From Fig.4(A) we can see that the material exhibits an open circuit potential of about 3.0 V, and the discharge profile is composed of two voltage plateaus at around 3.0 and 2.35 V, respectively. The discharge capacity is about 435 mA·h/g, corresponding to 4.3 mol of Li^+ inserted into CuV_2O_6. The first charge capacity is about 400 mA·h/g, which shows a good reversibility for lithium ion batteries. However, the second discharge profile changes to a short voltage plateau at about 2.6 V and the discharge capacity is reduced to about 350 mA·h·g^{-1}. The irreversible structural transition of the CuV_2O_6 nanowires in the first cycle has been regarded as an important factor for the capacity fading, reported by Wei *et al.*[7]. After the first cycle, the irreversible capacity

was immediately minimized, resulting in a stable Columbic efficiency of 97%. A discharge capacity of 130 mA·h/g was obtained after 70 cycles, indicating that the electrochemical cycle performance of the CuV_2O_6 nanowires is significantly superior over those reported previously[7,15,16]. The material was also charge-discharged with the current density of about 100 mA/g as shown in Fig.4(B). The first and the second discharge capacities are reduced to 351 and 274 mA·h/g, respectivity. After 40 cycles, the discharge capacity is decreased to 112 mA·h/g. The large capacity reduction shows a poor rate performance of the CuV_2O_6 nanowires.

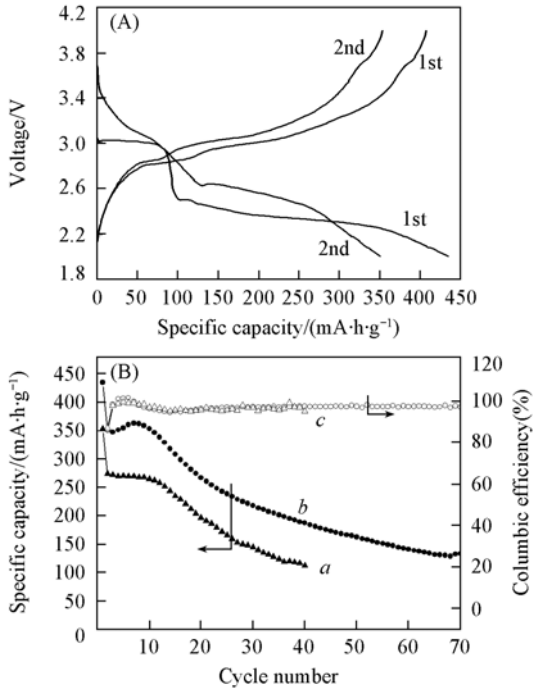

Fig.4 Charge-discharge potential profiles of the CuV_2O_6 nanowires during the first and the second cycles with the current density of 50 mA/g(A) and the cycles performance(*a, b*) and Coulombic efficiencies(*c*) of CuV_2O_6 nanowires at the current density of 50(*a*) and 100 mA/g(*b*), respectivity(B)

To examine the electrochemical kinetics behavior of the CuV_2O_6 nanowires, EIS is carried out at about 2.44 V during the first and the second discharge processes, separately. The corresponding Nyquist plots are shown in Fig.5.

As we know, the small intercept at high frequency corresponds to the internal resistance(R_s) of the battery cell, the semi-circle in the high frequency region is due to the resistance of SEI film(R_f), while the other one in the middle frequency region is due to the charge transfer resistance(R_{ct}), and the sloping line in the low frequency region corresponds to the diffusion of Li^+ ions in the electrode bulk, namely the Warburg impedance. The SEI film resistance and charge transfer resistance at 2.44 V can be obtained *via* fitting the Nyquist plots by the ZView package, separately. The results are listed in Table 1, which show that the SEI film has been evidently formed after the first cycle, and the charge transfer resistance changes little. The formation of the SEI film should be responsible

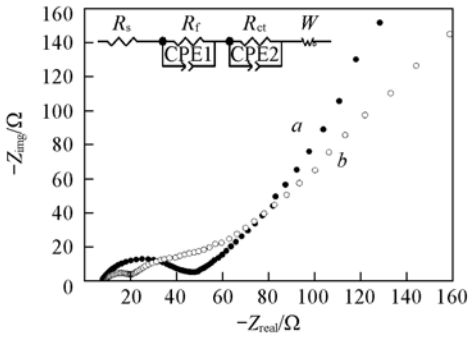

Fig.5 Nyquist plots at about 2.44 V during the first(*a*) and the second(*b*) discharge processes of CuV_2O_6 nanowires

Table 1 Electrochemical impedance parameters of CuV_2O_6 nanowires at about 2.44 V during the first and the second discharge processes

Cycle	R_s/Ω	R_f/Ω	R_{ct}/Ω	10^{14} D_{Li}/(cm^2·s^{-1})
1st	7.40	—	31.78	9
2nd	8.53	10.64	26.59	10.7

for the relatively fast capacity fading after the first cycle[17].

The ion diffusion coefficient of the materials at about 2.44 V during the first and the second discharge processes can be evaluated by the following equation[18]:

$$D_{Li} = 0.5R^2T^2 / S^2n^4F^4C^2\sigma^2 \quad (1)$$

where R is the gas constant, T the absolute temperature, S the surface area of the cathode electrode, n the number of electrons involved in the reaction(n=1), F the Faraday constant, and σ the Warburg factor, which obeys the following relationship:

$$Z_{real}=R_f+R_{ct}+\sigma\omega^{-1/2} \quad (2)$$

Fig.6 displays the linear fitting of Z_{real} *vs.* $\omega^{-1/2}$, from which the slope σ can be obtained. Using this value, the ion diffusion coefficient of the material can be calculated and the results are listed in Table 1, showing that the ion diffusion coefficient of the CuV_2O_6 nanowires is about 1.0×10^{-13} cm^2/s based on the EIS analysis. The low chemical diffusion coefficient could result in the poor rate performance of the CuV_2O_6 nanowires.

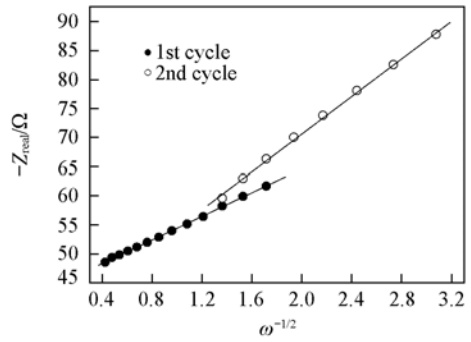

Fig.6 Linear fit of relationship between Z_{real} and $\omega^{-1/2}$ of CuV_2O_6 nanowires

4 Conclusions

α-CuV_2O_6 nanowires grown along [001] direction were prepared *via* a simple hydrothermal synthesis method. The electrochemical properties indicate a high discharge capacity in the first cycle, while show poor capacity retention and rate

performance. The low chemical diffusion coefficient could result in the poor electrochemical proformance of CuV_2O_6 nanowires. The reasons presented in this work are useful for the further modification and applications of vanadate compounds in rechargeable lithium batteries.

References

[1] Aidoudi F. H., Aldous D. W., Goff R. J., Slawin A. M. Z., Attfield J. P., Morris R. E., Lightfoot P., *Nat. Chem.*, **2011**, *3*, 801

[2] Nakano M., Shibuya K., Okuyama D., Hatano T., Ono S., Kawasaki M., Iwasa Y., Tokura Y., *Nature*, **2012**, *487*(7408), 459

[3] Marley P. M., Banerjee S., *Inorg. Chem.*, **2012**, *51*(9), 5264

[4] Devi S. S., Muthukumaran B., Krishnamoorthy P., *Ionics*, **2014**, *20*(12), 1783

[5] Li M. L., Yang X., Wang C. Z., Chen N., Hu F., Bie X. F., Wei Y. J., Du F., Chen G., *J. Mater. Chem. A*, **2015**, *3*, 586

[6] Zhu K., Yan X., Zhang Y. Q., Wang Y. H., Su A. Y., Bie X. F., Zhang D., Du F., Wang C. Z., Chen G., Wei Y. J., *Chem. Plus. Chem.*, **2014**, *79*, 447

[7] Wei Y. J., Ryu C. W., Chen G., Kim K. B., *Electrochem. Sol. Stat. Lett.*, **2006**, *9*(11), A487

[8] Pan A. Q., Zhang J. G., Cao G. Z., Liang S. Q., Wang C. M., Nie Z. M., Arey B. W., Xu W., Liu D. W., Xiao J., Li G. S., Liu J., *J. Mater. Chem.*, **2011**, *21*, 10077

[9] Zhang S. Y., Li W. Y., Li C. S., Chen J., *J. Phys. Chem. B*, **2006**, *110*, 24855

[10] Qiu C. G., Liu L.N., Du F., Yang X., Wang C. Z., Chen G., Wei Y. J., *Chem. Res. Chinese Universities*, **2015**, *31*(2), 270

[11] Zhang Y., Pan Y., Liu J., Wang G. L., Cao D. X., *Chem. Res. Chinese Universities*, **2015**, *31*(1), 117

[12] Wei Y. J., Nam K. W., Chen G., Ryu C. W., Kim K. B., *Sol. Stat. Ion.*, **2005**, *176*, 2243

[13] Cheng F. Y., Chen J., *J. Phys. Chem.*, **2011**, *21*, 9841

[14] Ma H., Zhang S. Y., Ji W. Q., Tao Z. L., Chen J., *J. Am. Chem. Soc.*, **2008**, *130*, 5361

[15] Cao X. Y., Xie J. G., Zhan H., Zhou Y. H., *Mater. Chem. Phys.*, **2006**, *98*(1), 71

[16] Cao J. Q., Wang X. Y., Tang A. P., Wang X., Wang Y., Wu W., *J. Alloy. Comp.*, **2009**, *479*, 875

[17] Shaju K. M., Rao G. V. S., Chowdari B. V. R., *Electrochim. Acta*, **2003**, *48*, 2691

[18] Liao X. Z., Ma Z. F., Gong Q., He Y. S., Pei L., Zeng L. J., *Electrochem. Commun.*, **2008**, *10*, 691